

Less Emphasis on Difficult Layer Regions: Curriculum Learning for Singularly Perturbed Convection-Diffusion-Reaction Problems

Yufeng Wang^{a,1}, Cong Xu^{a,c,2}, Min Yang^{a,*}, Jin Zhang^{b,3}

^a*School of Mathematics and Information Sciences, Yantai University, Yantai, China*

^b*Department of Mathematics, Shandong Normal University, Jinan, China*

^c*School of Computer Science and Technology, East China Normal University, Shanghai, China*

Abstract

Although Physics-Informed Neural Networks (PINNs) have been successfully applied to various differential equations, accurately solving perturbed convection-diffusion-reaction problems is still extremely challenging for PINNs. This paper investigates the source of the learning difficulties and finds that the rapid transition of potential solution in the layer region causes the failure of convergence. Based on this finding, we present a curriculum learning method that encourages neural networks to “prioritize the learning on easier non-layer regions”. The method helps PINNs to dynamically adjust the training data weights, speed up the learning procedure, and ultimately significantly improve the accuracy of the network approximation. Extensive evaluation on multiple typical model equations shows that the proposed approach accurately captures the resolution of the layer regions, and achieves multiple orders of magnitude lower root-mean-squared error than ordinary PINNs. We provide our PyTorch code at <https://github.com/WYu-Feng/CLPINN>.

Keywords: Convection-diffusion-reaction; Curriculum Learning; Physics-informed neural networks; Reweight; Singularly perturbed problem

1. Introduction

Deep learning has shown outstanding performance in various fields, including computer vision [34, 36, 37], natural language processing [3, 8], recommender system [7, 33], and so on. Recently, there has been a surge of interest in applying neural networks to solve differential equations, which yields the so-called physics-informed neural networks (PINNs) [1, 14, 20, 23, 25, 29]. The main idea of PINNs is to constrain the neural networks to minimize the specific loss function of the governing physical equation at the training

*Corresponding author: yang@ytu.edu.cn

¹Email: ytuyufengwang@163.com

²Email: congxueric@s.ytu.edu.cn

³Email: jinzhangalex@hotmail.com

sample points. As an interesting alternative to traditional numerical methods, PINNs do not require an underlying grid and can easily solve high-dimensional differential equations. Moreover, well-trained PINNs have good generalization ability and can quickly find new solutions outside the computational domain. However, there are still some differential equations that are extremely challenging for the current PINNs-based approach.

Singular perturbation equations appear in the modeling of various modern complicated processes, such as fluid flow at high Reynolds numbers [16], drift diffusion in semiconductor device modeling [28], and chemical reactor theory [27]. Very often the size of diffusion is smaller by several orders of magnitude compared to the size of convection and/or reaction, leading to sharp boundary and interior layers whose width, depending on the perturbation parameters, can be extremely small [30]. These layers are notoriously hard to capture accurately by common numerical methods [2, 6, 21, 32, 40, 39, 41].

In this paper, we observe that the prediction results of PINNs for singularly perturbed equations are far from satisfactory. The rapid change of latent solutions within the layer regions imposes great difficulties for the optimization of the neural networks. Ordinary PINNs, even using very dense sampling near the layer regions, cannot well capture the singular behaviors of the solutions. The training process fails to converge, and the resulted approximations show very large errors throughout the whole computational domain.

To address the difficulties encountered by PINNs, this paper presents a curriculum learning method for accurately solving singularly perturbed convection-diffusion-reaction equations. We believe that the large-scale variation in potential solutions makes it difficult for PINNs to manage the learning through layer and non-layer regions. To this end, we design a toy experiment to test this conjecture, and it turns out that naively discarding the training points near the boundary layer can enhance the performance of the network. Inspired by such finding, a novel learning approach is designed to help PINN automatically adjust its learning emphasis, prioritize “learning in easier non-layer regions”, and ultimately improve the accuracy of the neural network solution greatly. Extensive evaluation on multiple benchmark model equations shows that the proposed approach accurately captures the resolution of the layer regions, and achieves multiple orders of magnitude lower mean squared error than ordinary PINNs.

Our work falls under the category of curriculum learning methods [4, 13], which mimic human cognition and prioritize learning easier samples. Curriculum algorithms are often task-related, and existing ones have been developed primarily for applications such as computer vision [12, 18, 31] and natural language processing [22, 35]. The method in this paper, on the other hand, is proposed for PDE simulation and is different from previous methods in terms of algorithm design.

It is worth further emphasizing that the motivation of our approach is also significantly different from those of existing adaptive PINNs. Most existing adaptive algorithms prioritize the learning of harder regions, adding more sample points [9, 23, 38] or assigning large weights for difficult samples [11]. However, this paper discovers that for singular perturbation problems, learning should prioritize easier non-layer regions but downplay

harder layer ones.

The remainder of the paper is organized as follows. Section 2 gives the problem under study and introduces the basic notation of PINNs. Section 3 shows the difficulties encountered by ordinary PINNs in solving the singular perturbation equations and derives the motivation for our research. In Section 4, we provide the details of the curriculum learning algorithm developed in this paper. Section 5 gives comprehensive experimental results to demonstrate the efficiency of the proposed method. Finally, the conclusion is drawn in Section 5.

2. Problem Setup

Consider the following singularly perturbed convection-diffusion-reaction equation:

$$\mathcal{L}u := \epsilon \mathcal{L}_2 u + \mathcal{L}_1 u + \mathcal{L}_0 u = f(\mathbf{x}), \quad \mathbf{x} \in \Omega, \quad (2.1)$$

where Ω is a physical domain in \mathbb{R}^d , \mathcal{L}_k represents the differential operator of order k , $k = 0, 1, 2$, $f(\mathbf{x})$ denotes the source term, and the diffusion coefficient satisfies $0 < \epsilon \leq 1$. Further assume that the solution $u(\mathbf{x})$ satisfies the following boundary condition

$$\mathcal{B}u = g(\mathbf{x}), \quad \mathbf{x} \in \partial\Omega. \quad (2.2)$$

where \mathcal{B} is a well-defined differential operator for determining the condition on the admissible boundary $\partial\Omega$. When the diffusion coefficient ϵ is very small, the latent solution of the equation changes rapidly within some thin layers, posing a great challenge to the numerical simulation [6, 26].

For PINNs, the solution $u(\mathbf{x})$ is approximated by a neural network $u_\theta(\mathbf{x})$, where θ denotes the parameters of the network. Let

$$L_{phys}(\theta) = \frac{1}{N} \sum_{i=1}^N r_{phys}^2(\mathbf{x}_i; \theta) = \frac{1}{N} \sum_{i=1}^N [\mathcal{L}u_\theta(\mathbf{x}_i) - f(\mathbf{x}_i)]^2 \quad (2.3)$$

be the mean-squared physical residual loss of N training sample points in Ω , and

$$L_{bc}(\theta) = \frac{1}{M} \sum_{i=1}^M r_{bc}^2(\mathbf{x}_i; \theta) = \frac{1}{M} \sum_{i=1}^M [\mathcal{B}u_\theta(\mathbf{x}_i) - g(\mathbf{x}_i)]^2 \quad (2.4)$$

be the mean-squared boundary loss of M training sample points on $\partial\Omega$. All the samples constitute a training set X_{train} .

The neural network approximation $u_\theta(\mathbf{x})$ can be determined by solving the following optimization objective

$$\min_{\theta} L_{phys}(\theta) + \lambda L_{bc}(\theta), \quad (2.5)$$

where λ is a hyperparameter to balance the weights of the two loss terms.

Although PINNs have been successfully applied in solving many types of differential equations, we find the corresponding results for singularly perturbed equations are far from satisfactory. Next, we are to utilize a one-dimensional convection-diffusion equation to illustrate the dilemma encountered by ordinary PINNs.

3. Dilemma Encountered by PINNs

Consider the following one-dimensional convection-diffusion problem:

$$\begin{aligned} -\epsilon u_{xx} + (x - 2)u_x &= f(x), \quad x \in (0, 1), \\ u(0) &= u(1) = 0. \end{aligned} \tag{3.1}$$

where the diffusion coefficient ϵ is set as 10^{-3} , and the source term $f(x)$ is determined by the exact solution $u(x) = \cos(\pi x/2)(1 - \exp(2x/\epsilon))$. This problem has a boundary layer at $x = 0$.

3.1. Learning difficulties

Consider a four-layer fully connected neural network $u_\theta(x)$, where each intermediate layer has 20 neurons and Tanh is used as the activation function. The training set X_{train} consists of 2500 points uniformly sampled from the domain $(0, 1)$.

The network parameters are initialized by Normal Xavier or Uniform Xavier methods [10]. Two mainstream optimizers, Stochastic Gradient Descent (SGD) [5] and Adam [19], are utilized to solve the optimization objective (2.5), where the balance parameter λ is set to 1.

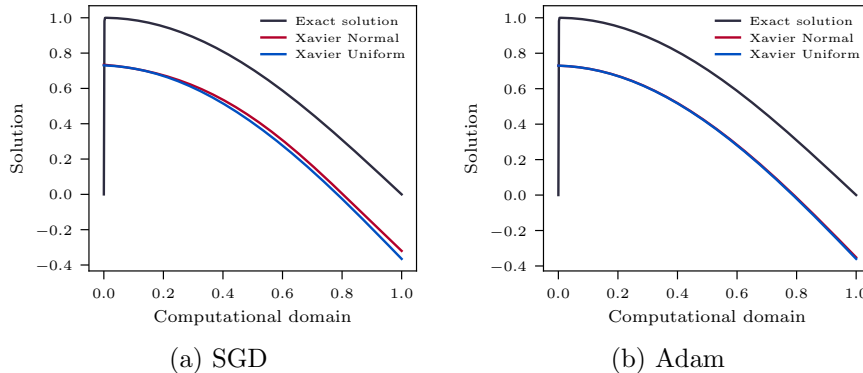


Figure 1: Predictions of PINN under two parameter initializations using SGD and Adam optimizers, respectively.

It can be observed from Figure 1 that the prediction $u_\theta(x)$ has very large errors throughout the computational domain, regardless of the initial or training methods used.

When we further plot the corresponding training loss curves (Figure 2), it is clear that the training loss of PINN fails to converge even after very long iterations.

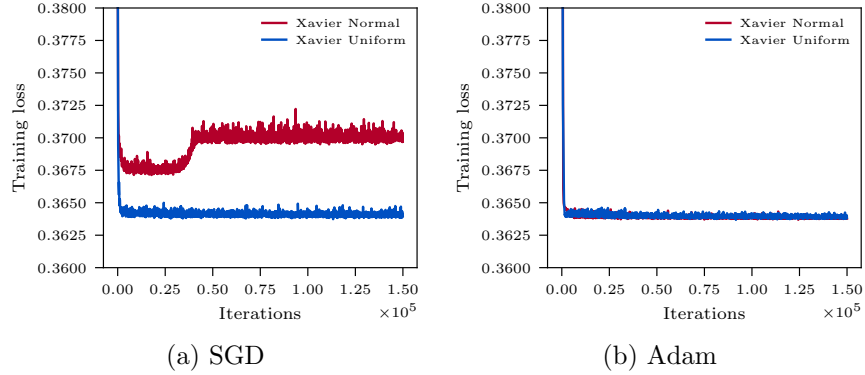


Figure 2: Training loss curves of PINN under various parameter initializations using SGD and Adam optimizations, respectively.

Let us further assume a very ideal case: the location of the layer is exactly know. A widely accepted experience from traditional numerical methods tells that the model performance might be improved by dense sampling near the layer. However, unfortunately, deep learning sometimes fall far from traditional methods. As can be seen from Figure 3, instead of improving PINN, encrypted sampling in the layer domain may lead to worse results.

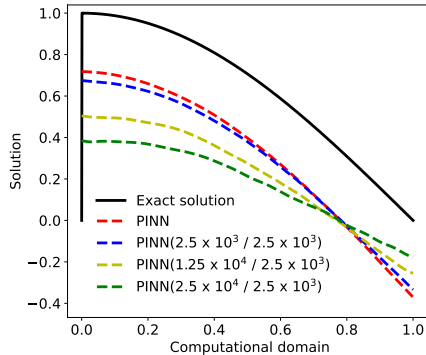


Figure 3: Predictions of PINN using a dense sampling in the layer domain, where 2500 points are sampled in the non-layer domain $(0.1, 1)$, and 2500, 12500, 25000 points are sampled in $(0, 0.1)$, respectively. For standard PINN, we apply a random sampling in $(0, 1)$.

3.2. The reason of the failure

The experiments in subsection 3.1 show that common PINNs cannot solve the singular perturbation equations well, even with dense sampling in the layer domain. This leads to a natural question what is the reason for such undesirable performance?

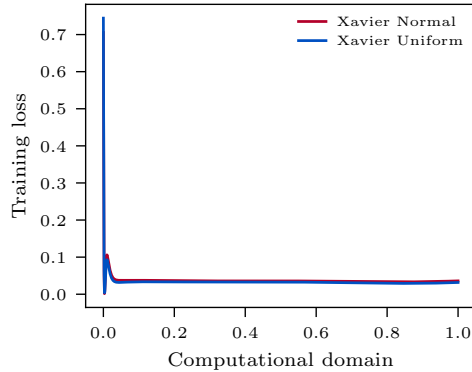


Figure 4: Training loss distribution of equation (3.1) under Normal Xavier or Uniform Xavier initializations using the Adam optimizer.

Notice that compared with ordinary equations, the latent solutions of singular perturbation equations exhibit sharp scale variations in different regions. In the narrow layer region the solution transits very rapidly, while in the wide non-layer region the solution varies more flatly and slowly. We argue that such large scale differences make PINNs difficult to balance the learning of data points from the layer and non-layer regions. The final loss distribution in Figure 4 shows the training losses for samples close to the boundary layer are much larger than those in the non-layer domain, which implies that the sharp layer domain is very difficult for PINNs to learn.

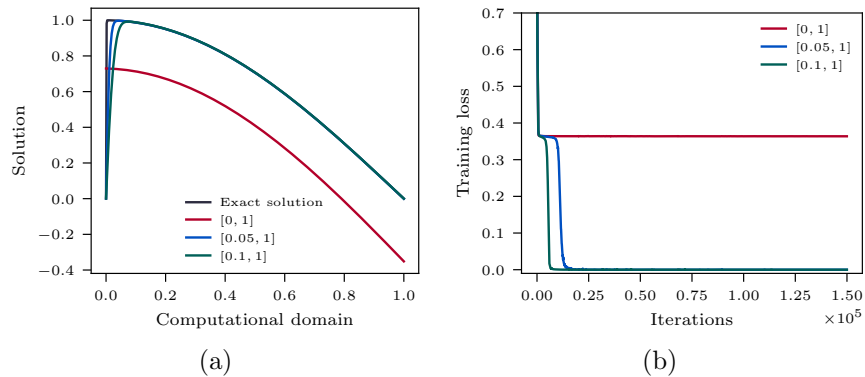


Figure 5: (a) Predictions of PINN after a rejection of the layer samples. (b) The corresponding training loss curves.

In order to reduce the learning difficulty of PINN, we conduct the following experiment. We only select samples from non-layer regions to build the training composed of samples in $(a, 1)$, where a is set to 0.05 and 0.1, respectively. It is surprising to see from Figure 5 that such a simple rejection of the layer samples leads to a significant improvement in prediction. This test has inspired us that “less emphasis on layer regions” may help to

raise the performance of PINNs in solving singularly perturbed problems.

Of course, naively rejecting samples from the layer regions will inevitably result in the loss of important physical information, thus cannot guaranteeing the high accuracy of the prediction. Moreover, the location of the layers is usually not known in practice. Therefore, in the next section, we are to present a curriculum learning algorithm that dynamically estimates the location of layers and adaptively adjusts the importance of the samples close to the layers.

4. The Proposed Curriculum Learning

From our previous experiments, we find that ordinary PINNs cannot well capture the complex characteristics of samples from different regions, thus leading to failure to converge. We argue that an ideal learning approach should treat samples of different regions differently, and imposes less importance to samples from difficult layer regions. In this section, we provide a curriculum learning algorithm, which mimics human learning and follows the principle of prioritizing easier samples, to raise the performance of PINNs in solving singularly perturbed problems.

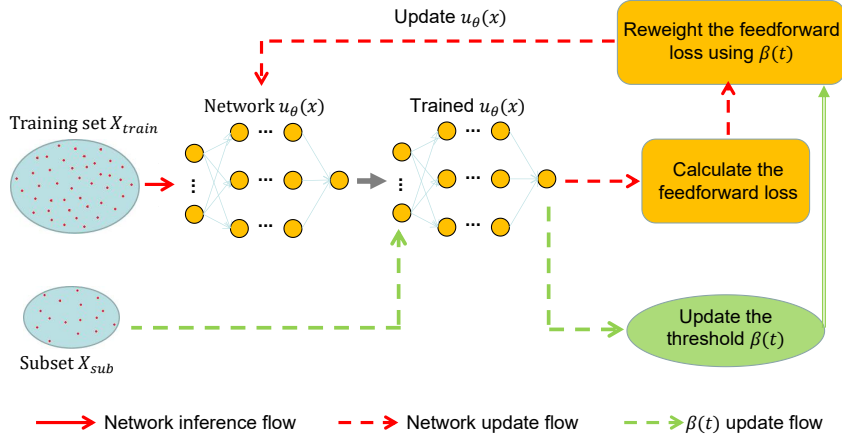


Figure 6: Curriculum learning framework. A fixed subset X_{sub} is used to update the threshold $\beta(t)$ at iteration step t . Then, the threshold $\beta(t)$ is employed to redetermine the weight of each sample, reducing the importance of the samples near the layers.

4.1. Proxy for layer location

Since the learning difficulty in layer and non-layer regions differs significantly, the first key step is to estimate the location of the layers. According to Figure 4, it can be found

that the layer region usually corresponds to a larger training loss. Therefore, we can take the feedforward training loss as a proxy to estimate the location of the layers. A larger loss implies that the corresponding sample is closer to the layer.

4.2. Sample reweighting

Recall that the optimization objective (2.3) is the average of the squared losses of all samples:

$$L_{phys}(\theta) = \frac{1}{N} \sum_{i=1}^N r_{phys}^2(\mathbf{x}_i; \theta),$$

which means that samples from different regions are of equal importance for learning.

In order to make PINN place less emphasis on the samples from the layer regions, we modify the optimization objective as follows

$$L_{phys}(\theta) = \frac{1}{\sum_{i=1}^N w(\mathbf{x}_i)} \sum_{i=1}^N w(\mathbf{x}_i) r_{phys}^2(\mathbf{x}_i; \theta), \quad (4.1)$$

where $w(\mathbf{x}_i)$ represents the importance of the sample. The closer the sample is to the layer, the less weight it has.

As discussed in Section 4.1, we do not know the exact locations of the layers and shall estimate them using the training losses that vary dynamically with iterations. Therefore, the weight of each sample should also be dynamically adjusted. To this end, we define

$$L_{phys}(\theta) = \frac{1}{\sum_{i=1}^N w(t, \mathbf{x}_i)} \sum_{i=1}^N w(t, \mathbf{x}_i) r_{phys}^2(\mathbf{x}_i; \theta), \quad (4.2)$$

where t denotes the iteration step. The sample weights in (4.2) are determined by

$$w(t, \mathbf{x}_i) = \begin{cases} 1, & \text{if } r_{phys}^2(\mathbf{x}_i) \leq \beta(t), \\ \frac{\beta(t)}{r_{phys}^2(\mathbf{x}_i)}, & \text{if } r_{phys}^2(\mathbf{x}_i) > \beta(t), \end{cases} \quad (4.3)$$

where $\beta(t)$ is a loss threshold that changes adaptively with iterations.

Intuitively, the formula (4.3) indicates that if the training loss of a sample is greater than $\beta^2(t)$, which implies that the point is close to the layer, then we give this sample a weight $\beta(t)/r_{phys}^2(\mathbf{x})$, which is less than 1. The larger the loss, the closer the sample is to the layer, and the smaller the corresponding weight. In this way, we not only guarantee the priority of samples from non-layer regions, but also preserve the necessary physical information of the layer regions.

4.3. Determine the threshold $\beta(t)$ with a training subset

Since the training loss of a desirable network model will gradually descent with iterations, then the threshold $\beta(t)$ should not be predetermined, but updated adaptively with the training process.

In order to reduce the computational cost, we will propose an algorithm to update $\beta(t)$ using a training subset. To this end, let X_{sub} be a randomly selected subset from the training set, which will be fixed during the training process.

First, notice that even with the same network structure, the training losses of different equations can vary greatly. Therefore, it is unlikely to directly determine a threshold that applies to all equations. Fortunately, we can observe from Figure 4 that the gradients of the training loss function are particularly steep near the layers. This could be true for most singular perturbation equations. Therefore, to ensure a better generalizability, we will use the gradient of the training loss for each sample in X_{sub} to determine the threshold $\beta(t)$.

Specifically, let G be a predefined constant. After the t -th iteration, for each $\mathbf{x} \in X_{sub}$, if $|\nabla_{\mathbf{x}} r_{phys}^2(\mathbf{x}; \theta)| < G$, which means that the sample is from non-layer regions, then we store the corresponding training loss into a clean memory bank. Finally, the maximum loss value in the memory bank is set as the threshold $\beta(t)$.

In fact, $\beta(t)$ can be regarded as an upper bound of the losses of non-layer samples in the subset. If the training loss of a sample from the training set exceeds this upper bound, then the corresponding sample is considered to belong to the layer regions.

Remark 1. *Since the training loss usually does not descent fast, especially in the late training period, to further reduce computational cost, one can update the threshold $\beta(t)$ every K iterations in practice. In our experiments, K is set as 50.*

Although weighted optimization algorithms have been extensively developed in the field of deep curriculum learning, the dynamic weighted objective proposed in (4.2) constitutes a novel function that is specifically designed for solving singular perturbation problems. The pseudo-code of the proposed approach is summarized in Algorithm 1.

5. Experiments

5.1. Experimental setup

To evaluate the performance of the proposed method, six benchmark convection-diffusion-reaction equations, including one 1-dimensional example, three 2-dimensional examples, and one 3-dimensional example, are considered. We implement our approach with PyTorch and run the experiments on a Intel Xeon CPU E5-2650 v3 platform with 14GB ROM and a RTX 3060 GPU. The balance weight λ in the optimization objective (2.5) is set to 1, the update frequency $K = 50$, and the constant G is set to 10 in the one-dimensional case and to 50 in the multidimensional cases. The subset X_{sub} is 1/5 of the size of the entire training set.

Algorithm 1 Pseudo-code of the curriculum learning for singularly perturbed problems

Require: Training set X_{train} , subset $X_{sub} \subset X_{train}$, predefined constant G , balance parameter λ , and update frequency K .

- 1: Initialize the iteration step $t = 0$.
 - 2: **for** each training step t **do**
 - 3: **if** t is divisible by K **then**
 - 4: Clean the memory bank M .
 - 5: **for** each $\mathbf{x} \in X_{sub}$ **do**
 - 6: **if** $|\nabla_{\mathbf{x}} r_{phys}^2(\mathbf{x}; \theta)| < G$ **then**
 - 7: Store the corresponding training loss into M .
 - 8: The threshold $\beta(t)$ is updated to the maximum value in M .
 - 9: Update the sample weights by (4.3).
 - 10: Update the network parameters based on the loss functions (2.4) and (4.2).
 - 11: $t++$.
-

We utilize six fully connected feedforward neural networks to solve different equations, respectively. All networks employ the Tanh function as the activation unit. Training process is performed using the Adam optimizer [19]. The specific network structures as well as the training parameters are specified in Table 1.

Table 1: Structures of neural networks and learning parameters.

Equation	Network depth	Network width	Optimizer	Batch size	Learning rate	Iterations
5.1	3	20	Adam	50	0.001	1.5×10^5
5.2	5	20	Adam	200	0.01	1.5×10^6
5.3	3	20	Adam	200	0.01	1×10^6
5.4	3	20	Adam	200	0.01	1×10^6
5.5	3	20	Adam	200	0.005	1.5×10^6
5.6	5	20	Adam	500	0.01	1×10^6

For the one dimensional equation, we employ a uniform sampling to construct the training set. For the multi-dimensional problems, In order to contain information within the layers with a few samples, we adopt a non-uniform sampling. Specifically, we first uniformly sample half of the training points, and then cryptographically sample around the points whose feedforward losses exceed the threshold $\beta(t)$, until the training set reaches the predefined size. The size of the training set for each equation is listed in Table 2.

If the exact solution is known, we quantify the performance of the prediction by using the Normalized Root-Mean-Squared Error (NRMSE):

$$\text{NRMSE} = \frac{\sqrt{\sum_{i=1}^n |u_{\theta}(x_i) - u(x_i)|^2}}{\sqrt{\sum_{i=1}^n |u(x_i)|^2}},$$

Table 2: Number of training points for different equations.

Equation	Interior samples	Boundary samples
5.1	2.5×10^3	2
5.2	2×10^4	4×10^2
5.3	2×10^4	4×10^2
5.4	2×10^4	4×10^2
5.5	2×10^4	4×10^2
5.6	3×10^5	6×10^4

where $u_\theta(x)$ and $u(x)$ represent the predicted and the exact solution, respectively, and n denotes the number of uniformly sampled test points, which is set to 1000 for one-dimensional equation, and 5000 for multi-dimensional equations.

5.2. 1d convection-diffusion equation

Consider the following two point problem:

$$\begin{aligned}
 -\epsilon u_{xx} + (x - 2)u_x &= f(x), \quad x \in (0, 1), \\
 u(0) &= u(1) = 0.
 \end{aligned}
 \tag{5.1}$$

where the source term $f(x)$ is chosen such that the exact solution $u(x) = \cos(\pi x/2)(1 - \exp(-2x/\epsilon))$. The solution of (5.1) is characterized by a boundary layer at $x = 0$.

We first plot the training loss curves of our approach and the conventional PINN in the case of $\epsilon = 1e - 9$. As demonstrated in Figure 7 (a), our method descends much faster than PINN in the early stage of training, and the corresponding training loss approaches 0 after about 4000 iterations. In contrast, PINN fails to converge even after a long period of iterations. It can be further observed from Figure 7 (b) and Figure 7 (c) that the prediction of our approach captures the boundary layer well and fits the exact solution much better over the entire computational domain, while the result of PINN differs significantly.

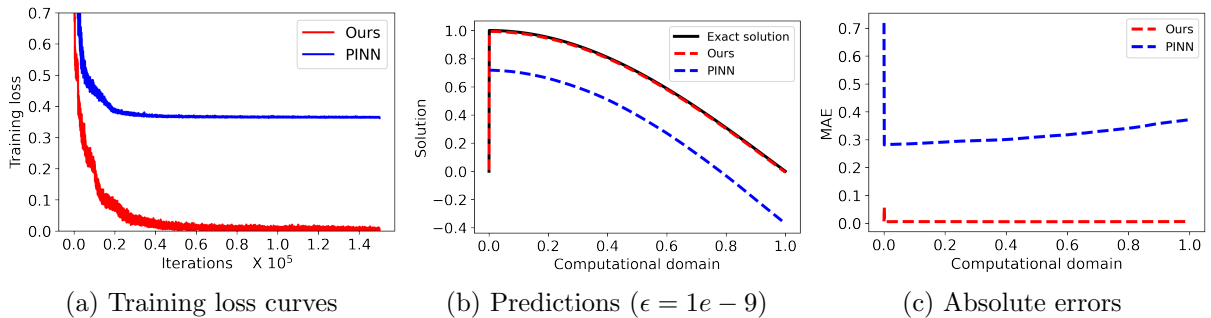


Figure 7: Comparison between our approach and PINN for one dimensional equation (5.1) with $\epsilon = 1e - 9$.

Further, we compare the normalized root-mean-squared errors of the two methods with more diffusion coefficients. It is obvious from Table 3 that for non-singularly perturbed

case ($\epsilon = 1$), both methods can produce satisfactory results of the same order of accuracy. However, for singularly-perturbed cases, the errors of our method is 3 orders of magnitude lower than those of PINN.

Table 3: Normalized root-mean-squared errors between the predicted and exact solutions of (5.1) under various diffusion coefficients.

Diffusion coefficient	Ours	PINN
$\epsilon = 1$	1.81×10^{-4}	1.83×10^{-4}
$\epsilon = 1e - 3$	1.41×10^{-4}	4.45×10^{-1}
$\epsilon = 1e - 6$	1.44×10^{-4}	4.54×10^{-1}
$\epsilon = 1e - 9$	1.47×10^{-4}	4.47×10^{-1}

5.3. 2d convection-diffusion-reaction equation with boundary layers

Consider the following two-dimensional problem [41]:

$$\begin{aligned}
 -\epsilon \Delta u + (3 - x_1 - x_2)u_{x_1} + 1.5u &= f, & \mathbf{x} \in \Omega = (0, 1)^2, \\
 u &= 0, & \mathbf{x} \in \partial\Omega.
 \end{aligned}
 \tag{5.2}$$

where $f(x)$ is chosen such that the exact solution

$$u = \left(\sin \frac{\pi x_1}{2} - \frac{e^{-(1-x_1)/\epsilon} - e^{-1/\epsilon}}{1 - e^{-1/\epsilon}} \right) \frac{(1 - e^{-x_2/\sqrt{\epsilon}})(1 - e^{-(1-x_2)/\sqrt{\epsilon}})}{1 - e^{-1/\sqrt{\epsilon}}}.$$

The solution of (5.2) is characterized by the presence of three layers, one at $x_1 = 1$, and two at $x_2 = 0$ and $x_2 = 1$.

It can be observed from Table 4 and Figure 8 that our method still performs well in capturing the behavior of the layers. The predictions only have a little oscillation at the boundary layer location. In contrast, the common PINN shows a considerable deviation from the truth.

Table 4: Normalized root-mean-squared errors between the predicted and exact solutions of (5.2) under various diffusion coefficients.

Diffusion coefficient	Ours	PINN
$\epsilon = 1e - 3$	4.67×10^{-4}	3.37×10^{-2}
$\epsilon = 1e - 6$	5.38×10^{-4}	5.31×10^{-1}
$\epsilon = 1e - 9$	5.35×10^{-4}	5.30×10^{-1}

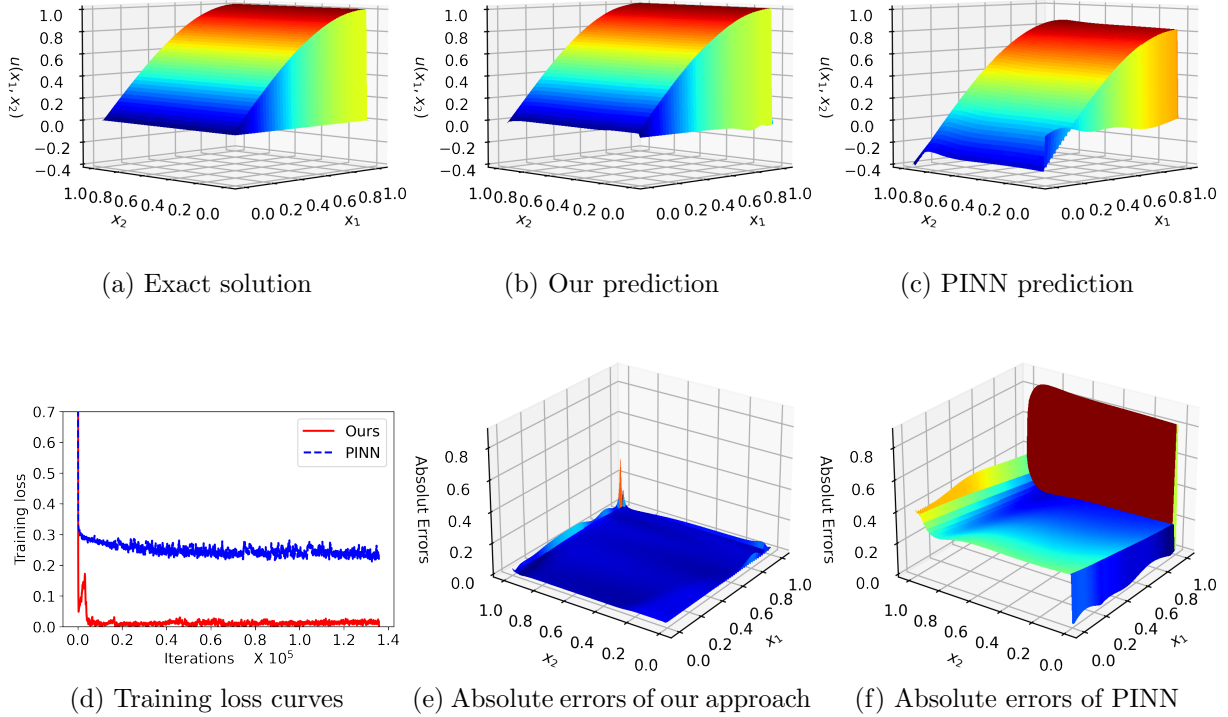


Figure 8: Comparison between our approach and PINN for equation (5.2) with $\epsilon = 1e - 9$.

5.4. 2d convection-diffusion equation with interior layers

This section is devoted to assessing the performance of the proposed approach in the presence of interior layers. To this end, consider [2]

$$\begin{aligned}
 -\epsilon \Delta u + \mathbf{b} \cdot \nabla u &= 0, \quad \mathbf{x} \in \Omega = (0, 1)^2, \\
 u &= \begin{cases} 1, & \text{if } x_2 = 0, \\ 1, & \text{if } x_1 = 0, x_2 \leq 1/5, \\ 0, & \text{elsewhere on } \partial\Omega, \end{cases} \quad (5.3)
 \end{aligned}$$

where the convection coefficient $\mathbf{b} = (1/2, \sqrt{3}/2)^T$. The latent solution of equation 5.3 presents both internal and external boundary layers. For most traditional numerical methods, non-physical oscillations are often observed near the interior layer caused by the joints of the conflicting discontinuous boundary conditions.

As can be seen from Figure (9), the internal layers are sharply captured by our approach with almost no overshooting/undershooting. In contrast, common PINN performs very poorly and its predictions are highly oscillatory. Moreover, in this example, our method is stable with respect to various ϵ . When ϵ changes from $1e - 3$ to $1e - 9$, there is no obvious oscillation appearing in the prediction results.

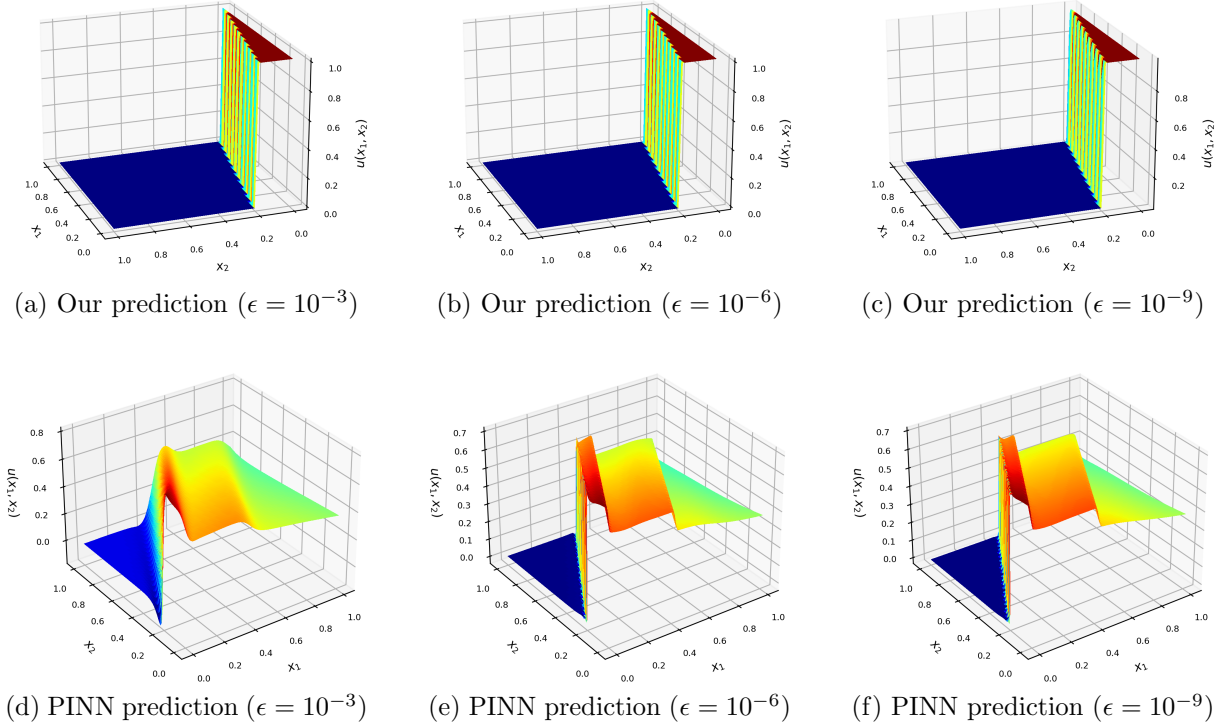


Figure 9: Comparison between our approach and PINN for equation (5.3) under various diffusion coefficients.

5.5. L-shaped domain

Consider the following convection-diffusion-reaction problem on a L-shaped domain [24]:

$$\begin{aligned}
 -\epsilon \Delta u + \mathbf{b} \cdot \nabla u + (3 + \sin(2\pi x_1 x_2))u &= 1 - (x_1 + x_2)/2, & \mathbf{x} \in \Omega &= (-1, 1)^2 / (-1, 0)^2, \\
 u &= 0, & \mathbf{x} \in \partial\Omega. &
 \end{aligned}
 \tag{5.4}$$

where the convection coefficient $\mathbf{b} = -(1 + 1/2 \sin(2\pi x_1), 2 - \cos(2\pi x_2))^T$, which results in boundary layers occurring at $x_1 = 0, 1$ and $x_2 = 0, -1$ [24].

From Figure (10), we can find that the boundary layers of the solution are well captured by our approach, with very slight overshooting/undershooting. In contrast, common PINN performs very poorly and its predictions are highly oscillatory. It is also noticeable that in this example, our method seems to degrade slightly in performance as ϵ gets smaller.

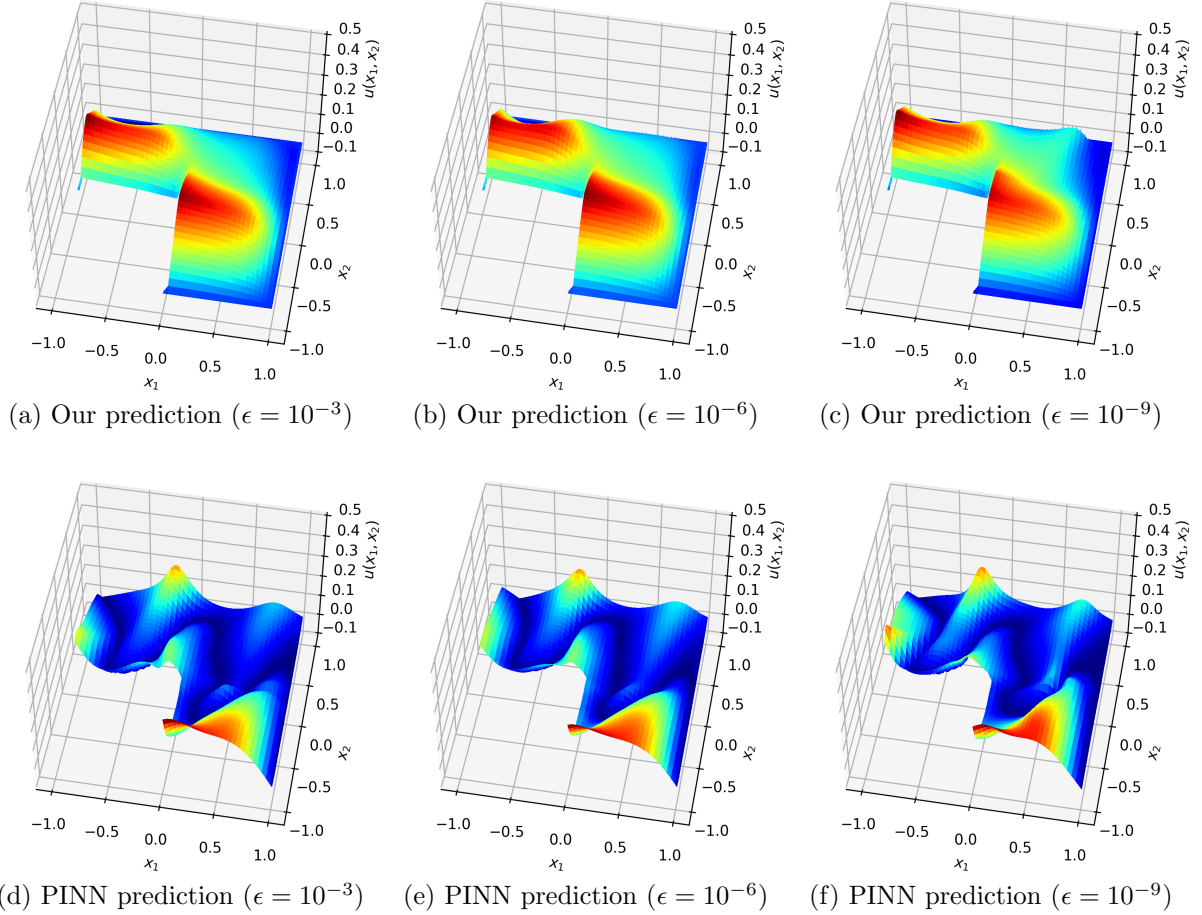


Figure 10: Comparison between our approach and PINN for L-shaped domain equation (5.4) under various diffusion coefficients.

5.6. Rotational flow

Consider the following problem [17]

$$-\epsilon \Delta u + \nabla \cdot (\mathbf{b}u) = 0, \quad \mathbf{x} \in \Omega = (0, 1)^2, \quad (5.5)$$

where the convection coefficient $\mathbf{b} = (1/2 - x_2, x_1 - 1/2)^T$, and the solution is prescribed along the slit $1/2 \times [0, 1/2]$ as follows

$$u(1/2, x_2) = \sin^2(2\pi x_2), \quad x_2 \in [0, 1/2].$$

The above equation describes the convection of a single component in a rotating flow field, where the axis of rotation passes through the center of the square domain.

Figure 11 shows that our method yields satisfactory predictions, while the results of PINN have unreasonably negative values near the boundary corners.

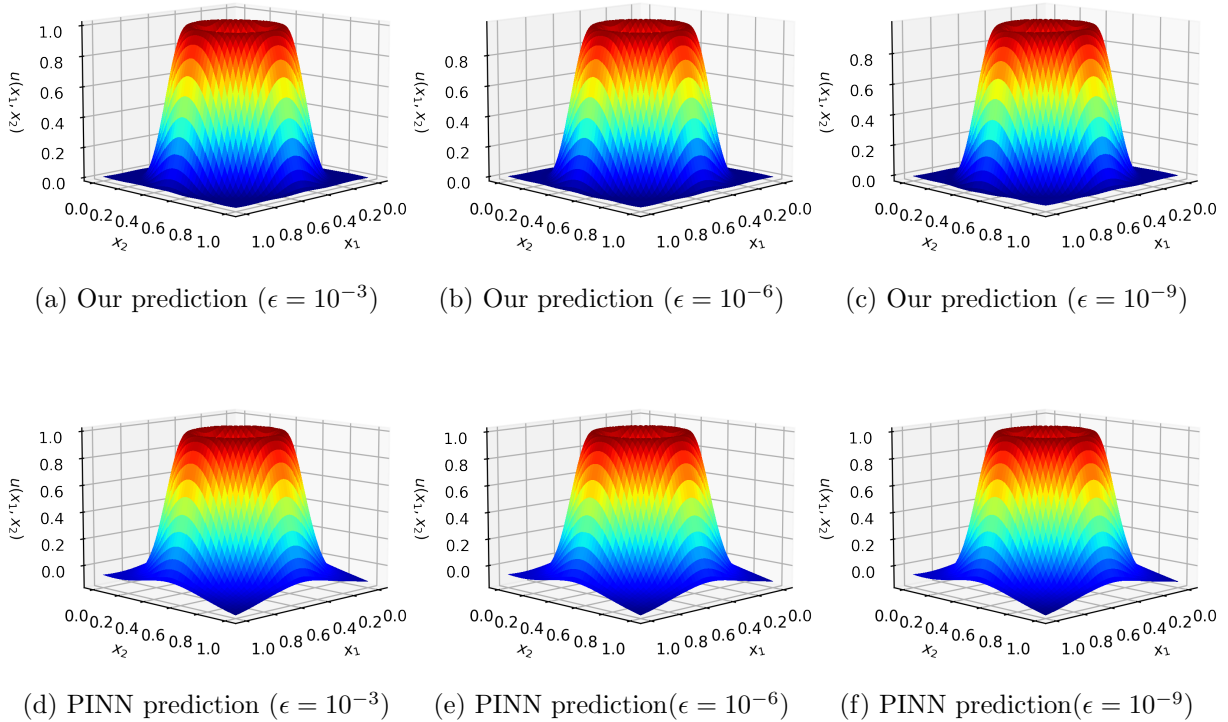


Figure 11: Comparison between our approach and PINN for rotational flow (5.5) under various diffusion coefficients.

5.7. 3d singularly perturbed convection-diffusion problem

For traditional numerical methods, the singular perturbation equations in three spatial dimensions are difficult to solve due to the huge computational cost. On the contrary, neural networks are more powerful in dealing with high-dimensional problems. To this end, consider the following three-dimensional convection-diffusion problem:

$$\begin{aligned} -\epsilon \Delta u + \mathbf{b} \cdot \nabla u &= f, & \mathbf{x} \in \Omega, \\ u &= 0, & \mathbf{x} \in \partial\Omega. \end{aligned} \quad (5.6)$$

where $\Omega = (0, 1)^3$, $\mathbf{b} = [1, 2, 1]^T$, and $f(x)$ is chosen such that the exact solution is given by

$$u = \sin(x_1)(1 - e^{-(1-x_1)/\epsilon})(1 - x_2)^2(1 - e^{-x_2/\epsilon})(1 - x_3)(1 - e^{-x_3/\epsilon})$$

The solution of (5.6) has three exponential layers at $x_1 = 1$, $x_2 = 0$ and $x_3 = 0$, respectively.

We give the errors and the corresponding computational time of our approach for solving equation (5.6). As can be seen from Table 5, the errors and computational time are very stable for various diffusion coefficients.

Table 5: Normalized root mean squared error and computational time of our approach for equation (5.6).

Diffusion coefficient	NRMSE	Cpu time(Second)
$\epsilon = 1e - 3$	4.37×10^{-3}	1.77×10^4
$\epsilon = 1e - 6$	4.46×10^{-3}	1.78×10^4
$\epsilon = 1e - 9$	4.43×10^{-3}	1.78×10^4

5.8. Sensitivity analysis

In our approach, there is an important hyperparameter G , which is used to quantify the magnitude of the gradients of the samples in the subset X_{sub} , and further helps to determine the threshold $\beta(t)$ for reweighting. In this subsection, we will study the effect of this hyperparameter.

To this end, we take the equation (5.1) with $\epsilon = 1e - 9$ as an example, and then apply our approach using $G = 1, 10, 20$ and 30 , respectively.

From Figure 12, we can find that the method is stable with respect to a large parameter G . Whether $G = 10, 20$ or 30 , the training process converges well, and the corresponding predictions are almost identical. On the contrary, $G = 1$ leads to unstable training and yields large prediction errors, which is mainly because a too small G cannot well distinguish the gradients from layer or non-layer regions.

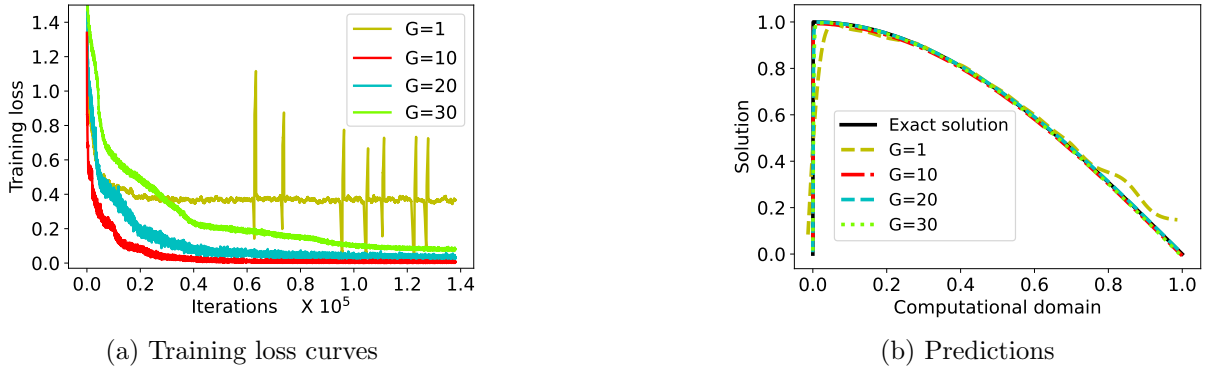


Figure 12: Sensitivity studies for the hyperparameter G .

6. Conclusion

Singularly perturbed problems have a multi-scale nature in the sense that the solutions have their own specific scales in different parts, and standard PINNs applied to such problems produce unsatisfactory predictions. This paper presented a curriculum learning approach to enhance the performance of PINNs in solving singularly perturbed convection-diffusion-reaction equations. The feedforward training loss is taken as a surrogate to

estimate whether a sample is close to layers or not. For those samples near layers, their weights are adaptively adjusted in the optimization objective, i.e., the closer to layers, the smaller the weights are. In this way, the network is able to automatically adjust its learning emphasis and prioritize learning in easier non-layer domains. Numerical experiments on typical convection-diffusion-reaction equations have demonstrated the efficiency of the proposed method.

Although the paper is concerned with singularly perturbed convection-diffusion-reaction problems, the proposed approach can be readily extended to other singular perturbation problems with multiscale natures. In addition, our approach also suggests a general idea for deep learning of singularly perturbed problems, and more powerful algorithms could be explored along this direction.

References

- [1] Ainsworth M. & Dong J. Galerkin neural networks: a framework for approximating variational equations with error control, *SIAM J. Sci. Comput.* 43(2021), A2474–A2501.
- [2] Ayuso B. & Marini L. Discontinuous Galerkin methods for advection-diffusion-reaction problems. *SIAM J. Numer. Anal.* 47(2009), 1391–1420.
- [3] Bahdanau D., Cho K. & Bengio Y. Neural machine translation by jointly learning to align and translate. In *International Conference on Learning Representations (ICLR)*, 2015.
- [4] Bengio Y., Louradour J., Collobert R. & Weston J. Curriculum learning. In *International Conference on Machine Learning (ICML)*, 2009.
- [5] Bottou L. Stochastic gradient learning in neural networks. In *Proceedings of Neuro-Nimes*, 1991.
- [6] Brooks A. & Hughes T. Streamline upwind/Petrov-Galerkin methods for advection dominated flows In *Proc. Third Internat. Conf. on Finite Element Methods in Fluid Flow*, 1980.
- [7] Cao J., Lin X., Cong X., Ya J., Liu T. & Wang B. DisenCDR: learning disentangled representations for cross-domain recommendation. In *ACM SIGIR Conference on Research and Development in Information Retrieval (SIGIR)*, 2022.
- [8] Csaky R., Purgai P. & Recski G. Improving neural conversational models with entropy-based data filtering. In *Annual Meeting of the Association for Computational Linguistics (ACL)*, 2019.

- [9] Daw A., Bu J., Wang S., Perdikaris P. & Karpatne A. Rethinking the importance of sampling in physics-informed neural networks, arXiv:2207.02338, 2022.
- [10] Glorot X. & Bengio Y. Understanding the difficulty of training deep feedforward neural networks. In *International Conference on Artificial Intelligence and Statistics (AISTATS)*, 2010.
- [11] Gu Y., Yang H. & Zhou C. Selectnet: self-paced learning for high dimensional partial differential equations. *J. Comput. Phys.* 441(2021), 110444.
- [12] Guo S., Huang W., Zhang H., Zhuang C., Dong D., Scott M.R. & Huang D. Curriculumnet: weakly supervised learning from large-scale web images. In *Proceedings of the European Conference on Computer Vision (ECCV)*, 2018.
- [13] Hacoen G. & Weinshall D. On the power of curriculum learning in training deep network. In *International Conference on Machine Learning (ICML)*, 2019.
- [14] Han J., Jentzen A. & E W. Solving high-dimensional partial differential equations using deep learning. In *Proceedings of the National Academy of Sciences*, 2018.
- [15] Hanna J.M., Aguado J.V., Comas-Cardona S., Askri R. & Borzacchiello D. Residual-based adaptivity for two-phase flow simulation in porous media using physics-informed neural networks, *Comput. Methods Appl. Mech. Engrg.* 396(2022), 115100.
- [16] Hirsch C. *Numerical Computation of Internal and External Flows: The Fundamentals of Computational Fluid Dynamics*. Butterworth-Heinemann, Elsevier, 2007.
- [17] Hughes T., Scovazzi G., Bochev P. & Buffa A. A multiscale discontinuous Galerkin method with the computational structure of a continuous Galerkin method. *Comput. Methods Appl. Mech. Engrg.* 195(2006), 2761–2787.
- [18] Jiménez-Sánchez A., Mateus D., Kirchoff S., Kirchoff C., Biberthaler P., Navab N., González Ballester M. & Piella G. Medical-based deep curriculum learning for improved fracture classification. In *International Conference on Medical Image Computing and Computer-Assisted Intervention (MICCAI)*, 2019.
- [19] Kingma D. & Ba J. ADAM: a method for stochastic optimization. In *International Conference on Learning Representations (ICLR)*, 2015.
- [20] Krishnapriyan A., Gholami A., Zhe S., Kirby R. & Mahoney M. Characterizing possible failure modes in physics-informed neural networks. In *Advances in Neural Information Processing Systems (NIPS)*, 2021.
- [21] Lin R., Ye X., Zhang S. & Zhu P. A weak Galerkin finite element method for singularly perturbed convection-diffusion-reaction problems. *SIAM J. Numer. Anal.* 56(2018), 1482–1497.

- [22] Liu X., Lai H., Wong D. & Chao L. Norm-based curriculum learning for neural machine translation. In *Annual Meeting of the Association for Computational Linguistics (ACL)*, 2020.
- [23] Lu L., Meng X., Mao Z. & Karniadakis G.E. DeepXDE: A deep learning library for solving differential equations, *SIAM Review* 63(2021), 208–228.
- [24] Ludwig L. & Roos H.G. Convergence and supercloseness of a finite element method for a singularly perturbed convection-diffusion problem on an L-shaped domain, *IMA J. Numer. Anal.* 36(2016), 1261–1280.
- [25] Matthey R. & Ghosh S. A novel sequential method to train physics informed neural networks for allen cahn and cahn hilliard equations, *Comput. Methods Appl. Mech. Engrg.* 390(2022), 114474.
- [26] Miller J., O’Riordan E. & Shishkin G., *Fitted Numerical Methods for Singular Perturbation Problems*. World Scientific, Singapore City, 1996.
- [27] Miller J. *Singular Perturbation Problem in Chemical Physics: Analytic and Computational Methods*. John Wiley and Sons, New York, 1997.
- [28] Polak S., Denheijer C. & Schilders W. Semiconductor device modelling from the numerical point of view, *Int. J. Numer. Methods Eng.* 24(1987), 763–838.
- [29] Raissi M., Perdikaris P. & Karniadakis G.E. Physics informed neural networks: A deep learning framework for solving forward and inverse problems involving nonlinear partial differential equations, *J. Comput. Phys.* 378(2019), 686–707.
- [30] Roos H.G., Stynes M. & Tobiska L. *Robust Numerical Methods for Singularly Perturbed Differential Equations*, volume 24 of *Springer Series in Computational Mathematics*. Springer-Verlag, Berlin, 2008.
- [31] Sarafianos N., Giannakopoulos T., Nikou C. & Kakadiaris I. Curriculum learning of visual attribute clusters for multi-task classification, *Pattern Recognit.* 80(2018), 94–108.
- [32] Stynes M. & Tobiska L. The SDFEM for a convection-diffusion problem with a boundary layer: optimal error analysis and enhancement of accuracy, *SIAM J. Numer. Anal.* 41(2003), 1620–1642.
- [33] Wang W., Lin X., Feng F., He X., Lin M. & Chua T. Causal representation learning for out-of-distribution recommendation. In *International World Wide Web Conferences (WWW)*, 2022.

- [34] Wang Y., Li D., Li X. & Yang M., PC-GAIN: Pseudo-label conditional generative adversarial imputation networks for incomplete data, *Neural Networks* 141(2021), 395–403.
- [35] Xu B., Zhang L., Mao Z., Wang Q., Xie H. & Zhang Y. Curriculum learning for natural language understanding. In *Annual Meeting of the Association for Computational Linguistics (ACL)*, 2020
- [36] Xu C., Li X. & Yang M., An orthogonal classifier for improving the adversarial robustness of neural networks, *Information Sciences* 591(2022), 251–262.
- [37] Xu C. & Yang M. Adversarial momentum-contrastive pre-training, *Pattern Recog. Lett.* 160(2022), 172–179.
- [38] Zeng S., Zhang Z., & Zou Q. Adaptive deep neural networks methods for high-dimensional partial differential equations, *J. Comput. Phys.* 463(2022), 111232.
- [39] Zhang J. & Liu X. Analysis of SDFEM on Shishkin triangular meshes and hybrid meshes for problems with characteristic layers, *J. Sci. Comput.* 68(2016), 1299–1316.
- [40] Zhang J., Liu X. & Yang M., Optimal order L2 error estimate of SDFEM on Shishkin triangular meshes for singularly perturbed convection-diffusion equations, *SIAM J. Numer. Anal.* 54(2016), 2060–2080.
- [41] Zhang J. & Stynes M. Supercloseness of continuous interior penalty method for convection–diffusion problems with characteristic layers, *Comput. Methods Appl. Mech. Engrg.* 319(2017), 549–566.